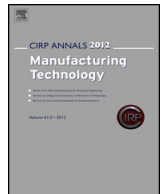




Contents lists available at SciVerse ScienceDirect

CIRP Annals - Manufacturing Technology

journal homepage: <http://ees.elsevier.com/cirp/default.asp>

# Machinability and surface integrity of Nitinol shape memory alloy

Yuebin Guo (2)<sup>a,\*</sup>, Andreas Klink<sup>b</sup>, Chenhao Fu<sup>a</sup>, John Snyder<sup>a</sup><sup>a</sup>Department of Mechanical Engineering, The University of Alabama, Tuscaloosa, AL 35487, USA<sup>b</sup>Laboratory for Machine Tools and Production Engineering (WZL), RWTH Aachen University, 52074 Aachen, Germany

## ARTICLE INFO

**Keywords:**  
Machinability  
Surface integrity  
Shape memory alloy

## ABSTRACT

Nitinol shape memory alloys have wide applications in medical devices and actuators. However, the unique mechanical properties including superelasticity, high ductility, and severe strain-hardening make Nitinol exceedingly difficult to cut. This work determines dynamic mechanical behaviors of Nitinol in cutting. It is found that the very high strength and specific heat are responsible for large flank wear and fast tribo-chemical crater wear, respectively. The austenitic white layer in cutting is caused by deformation, while the twinned martensitic white layer is caused by quenching in EDM. Alloying from tools is negligible in cutting but unavoidable even in finish EDM trim cut.

© 2013 CIRP.

## 1. Introduction

Nitinol, a nearly equiatomic nickel–titanium shape memory alloy, has wide applications in cardiovascular stents, micro-actuators, and high damping devices [1]. The microstructure characteristic of Nitinol is that it is in a martensitic phase at lower temperatures, but in an austenitic phase at elevated temperatures. Nitinol exhibits two unique mechanical behaviors: thermal shape memory and superelasticity [2], which are illustrated in the stress–strain–temperature diagram in Fig. 1. The phase transformation that occurs in Nitinol is dependent on the start and finish thermal transitions of the austenite and martensite crystalline phases. It is important to understand the diffusionless transformation to predict the mechanical behavior.

Fig. 1 shows the path that thermal shape memory takes place. Assuming Nitinol initially is in an austenitic state at the origin point  $O$ . With no applied stress as Nitinol is cooled along path  $O \rightarrow A$  below martensite finish temperature ( $M_f$ ), complete transformation from austenite to martensite (twinned) will occur. The material is deformed through reorientation and detwinning of martensite along path  $A \rightarrow B$ . Then, load releasing on path  $B \rightarrow C$  will cause elastic unloading of the reoriented detwinned martensite and the material stays deformed. On heating above the austenite finish temperature ( $A_f$ ), the material transforms from martensite to austenite and recovers the pseudoplastic deformation “remembering” its former shape.

The austenitic Nitinol can be loaded along the path  $O \rightarrow E$  (Fig. 1) above the austenite finish temperature ( $A_f$ ) through a stress-induced transformation to martensitic state. A large elastic strain up to 11% can be achieved. Upon unloading along the path  $E \rightarrow O$ , the material will transform back to austenitic state and the superelastic deformation will be recovered, demonstrating a hysteresis loop in the stress–strain diagram.

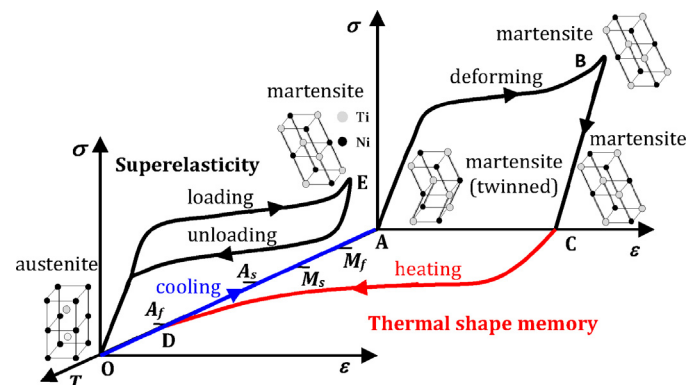


Fig. 1. Stress–strain–temperature diagram of Nitinol.

Due to the shape memory and superelasticity effects, high ductility, and strong work hardening, short tool life and burr formation are critical issues in cutting of Nitinol [3–5]. Shaping is mostly achieved by laser machining [6] and EDM [7]. The major drawback of laser machining is the high temperature induced thermal damage to the machined surface, which leads to significant reduction of fatigue life. Additional finishing is often required to remove the heat-affected zone (HAZ). Furthermore, the achievable aspect ratios are limitations of laser machining.

Milling is a versatile alternative cutting process for making Nitinol structures with large aspect ratios or small batch manufacturing. However, very little research has been done on process mechanics and surface integrity due to the very complex coupling between phase transformation and loading (large strain, high strain rate, and high temperatures) in cutting.

The objectives of this study are to: (1) investigate the dynamic material property at high rates in compression of biomedical  $Ni_{50.8}Ti_{49.2}$  Nitinol alloy, (2) explore tool wear mechanisms, and (3) investigate the process-induced surface integrity and edge quality.

\* Corresponding author.

In addition, surface integrity by milling vs. electrical discharge machining (EDM) is compared.

## 2. Dynamic mechanical properties of Ni<sub>50.8</sub>Ti<sub>49.2</sub> Nitinol alloy

Nitinol Ni<sub>50.8</sub>Ti<sub>49.2</sub> (50.8 at.% Ni–49.2 at.% Ti) is common for biomedical applications and is known to have an elastic recoil of up to 10–11%. In order to understand the process mechanics and process-induced surface integrity by cutting, both quasi-static and Split-Hopkinson pressure bar (SHPB) compression tests were conducted to obtain dynamic stress–strain behavior. The material was heat treated in a salt bath at 505 °C for 45 s to achieve superelastic properties at room temperature. The sample dimensions for quasi-static and Split-Hopkinson pressure bar (SHPB) compression tests are 12.5 mm height × 12.5 mm diameter and 6.35 mm height × 6.35 mm diameter, respectively. Testing shows very good repeatability of stress–strain curve at each loading. Fig. 2 shows the distinctive austenite loading/plateau/martensite loading which is only seen on the quasi-static stress–strain curve. The ultimate compressive strength (UCS), the highest stress on the stress–strain curves, reaches up to 2.3 GPa at quasi-static shearing. Fig. 2 also shows that flow stress is very sensitive to strain rate. At moderate rates, the superelastic plateau region does not occur, and the UCS reaches up to 3.0 GPa. However, when the rate is further increased past a certain range the UCS starts to reduce but is still as high as 1.8 GPa, while the failure plastic strain increases up to 0.2 due to significant thermal softening resulted from adiabatic shearing. The phenomena is attributed to the very high specific heat (837 J/kg K) of Nitinol compared to Ti–6Al–4V (527 J/kg K) and IN 718 (435 J/kg K) alloys, which produces higher temperatures and makes adiabatic shearing occur much more easily in high rate deformations. These unique mechanical behaviors demonstrate that Nitinol is much more difficult to machine than Ti/Ni-based superalloys.

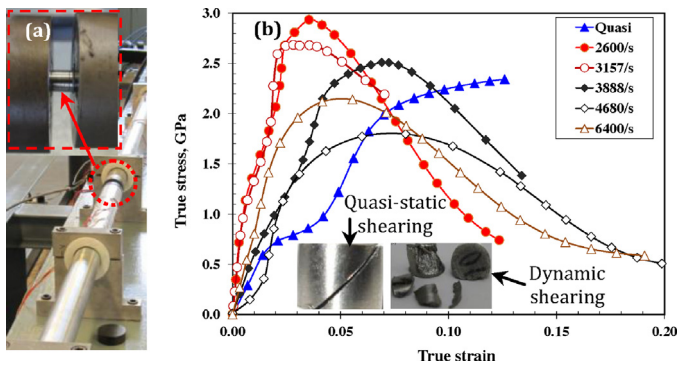


Fig. 2. Dynamic mechanical behavior of Ni<sub>50.8</sub>Ti<sub>49.2</sub> Nitinol alloy: (a) experimental setup and (b) rate dependent stress–strain curve.

## 3. Machinability by milling

### 3.1. Tool wear characteristics

Milling of Nitinol Ni<sub>50.8</sub>Ti<sub>49.2</sub> bars (12.5 mm diameter) was carried out on a CNC milling machine with general purpose synthetic coolant. The (Ti, Al) N/TiN coated carbide inserts (Fig. 3) are preferable for cutting Nitinol alloys in terms of cost [3]. Multiple cutting passes were performed at each milling condition. The representative cutting edge is characterized by the very large flank wear and coating flaking as well as some degree of notching and microchipping (Fig. 3). At higher feed rates, flank wear increases due to the increased mechanical load. The higher the feed rate, the larger flank wear. Compared to conventional metals, tool life is much shorter in milling of Nitinol. The very high strength up to 3 GPa of the material imposes significant mechanical loading on the tool/work interface, which results in an exceedingly strong

adhesion on the flank face. In addition, the very high specific heat of Nitinol is expected to produce high cutting temperatures to induce tribo-chemical dissolving of tool coating and the resulted large coating flaking.

### 3.2. Surface integrity characterization

**Surface and edge finish:** Surface topography was measured using a laser profilometer with a sampling length of 3 mm. The representative (repeatable) surface topography under the well-controlled process conditions is shown in Fig. 4. The dependence of  $R_a$  on feed rate shows that the lowest  $R_a$  can be produced at a certain feed rate. The smallest feed rate (50 mm/min) produces  $R_a$  0.40  $\mu$ m. When feed rate increases up to 200 mm/min,  $R_a$  reaches the lowest value of 0.19  $\mu$ m. The further increase of feed rate significantly increases  $R_a$  to 1.66  $\mu$ m in the concerned milling conditions. The trend shows that large feed rates significantly increase  $R_a$ , but a very small feed rate does not yield small  $R_a$ . A similar  $R_a$  trend on feed rate also occurred in turning of Nitinol [3]. By correlating the flank wear with  $R_a$ , it is found that the increase of flank wear increases  $R_a$  in general due to the accumulated tool/material adhesion. However, the lowest flank wear not necessarily produces smallest  $R_a$ . Machining dynamics and uncertainty could be responsible for the phenomena.

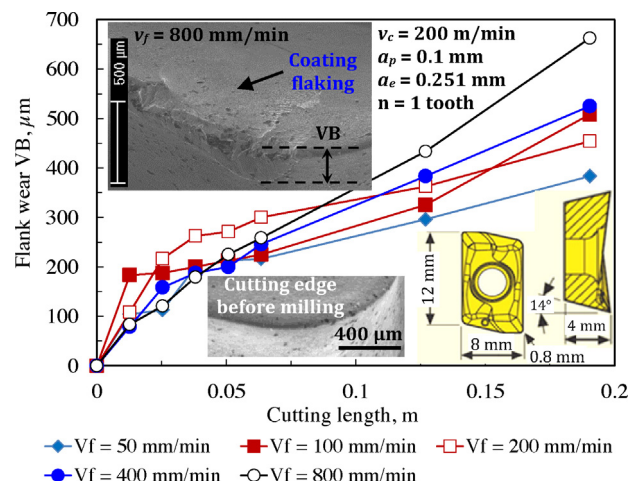


Fig. 3. Tool wear patterns with regard to feed rate.

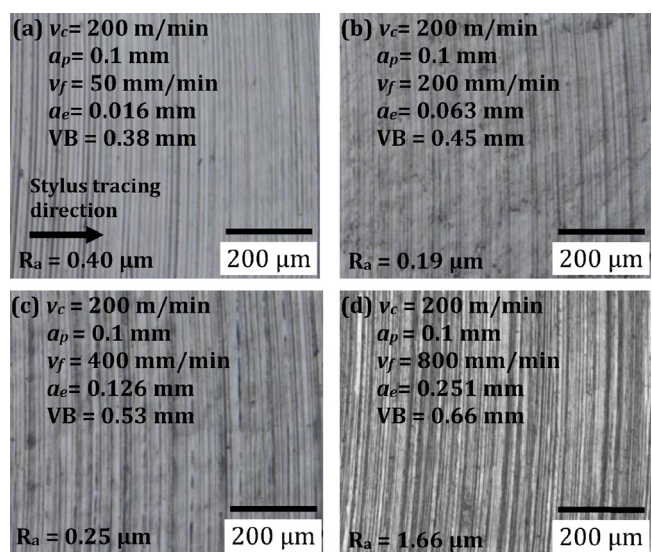


Fig. 4. Representative surface topography dependence on feed rate.

One characteristic of the machined surfaces is large exit burrs (Fig. 5). The burr formation experiences four stages: initiation, initial development, pivoting point, and final development [8]. When the feed rate increases, large cutting force is expected to

Download English Version:

<https://daneshyari.com/en/article/10674369>

Download Persian Version:

<https://daneshyari.com/article/10674369>

[Daneshyari.com](https://daneshyari.com)